

## Supplementary Methods

### Plasmid preparations

The pRS316RAD4cmyc plasmid (for the *RAD4* strain) was generated by amplification of the *RAD4* Open Reading Frame (ORF) complemented by 190bp upstream and 282bp downstream of the coding sequence on genomic DNA with the primers pRS-RAD4-NotI-F and pRS-RAD4-EcoRI-R. The PCR product was inserted NotI/EcoRI into pRS316 (see **Supplementary Table S2** for primers used in the study). Finally, the cmc tag was inserted in between NdeI/EcoRI right before the STOP codon of *RAD4* by overlapped PCR using pRS-RAD4-2995-NdeI-F, pRS-RAD4-cmyc-R, pRS-RAD4-cmyc-F and pRS-RAD4-EcoRI-R. The previous intermediate plasmid was used as template. The pRS316RAD4(F95P/V98P)cmc plasmid (*rad4-PP*) was obtained by the QuikChange (QuikChange Site-Directed Mutagenesis Kit from Stratagene) mutagenesis procedure using the primers RAD4(F95P+V98P)-F and RAD4(F95P+V98P)-R with the pRS316RAD4cmc plasmid as template. The pRS316RAD4(W649A/L652A/L656A)cmc (*rad4-AAA*) and pRS316RAD4(F95P/V98P/W649A/L652A/L656A)cmc (*rad4-PPAAA*) plasmids were both obtained by overlapped PCR using the primers pRS-RAD4-1742-BglIII-F(L), RAD4I(W649AL652AL656A)-R, RAD4(W649AL652AL656A)-F and pRS-RAD4-EcoRI-R with pRS316RAD4cmc plasmid as template. The PCR product was inserted BglIII/EcoRI into either pRS316RAD4cmc or pRS316RAD4(F95P/V98P)cmc respectively.

### NMR samples

For the NMR chemical shift titration studies of Rad4 and Rad34 segments with Tfb1PH, either unlabeled Rad4<sub>76-115</sub> or unlabeled Rad34<sub>41-63</sub> was added to a sample containing 0.5 mM of <sup>15</sup>N-labeled Tfb1PH in NMR buffer to a final ratio of 1:1. These studies were performed in 20

mM sodium phosphate buffer pH 6.5, 1 mM EDTA, 1 mM DTT (NMR buffer) with 90% $\text{H}_2\text{O}$ /10% $\text{D}_2\text{O}$ .

For the NMR competition experiment of Rad4<sub>76-115</sub> and Rad2<sub>642-690</sub>, a sample containing 0.5 mM  $^{15}\text{N}$ -labeled Rad4<sub>76-115</sub> in NMR buffer was used. To this sample, unlabeled Tfb1PH was added to a final concentration of 0.4 mM. In a second addition, unlabeled Rad2<sub>359-383</sub> was added to a final concentration of 1.5 mM.

The samples were recorded at 25°C on a Varian Inova 600 MHz spectrometer.

### **Protein expression levels in yeast**

To determine the expression level of the Rad4 protein and its mutants, normal protein levels were too low to detect when expressed from their endogenous promoters. Therefore, Rad4 and all mutants were cloned into the overexpression vector pVT-101u, which is under the control of the ADH promoter. The genes were inserted XhoI/BamHI and a myc-tag was fused on their C-terminus. Yeast cells were grown in 15 mL of minimal media to  $\text{OD}_{595} = 0.8-1.0$  and centrifuged. The pellets were resuspended and total protein extractions were carried out as previously described (56). The protein extracts (20  $\mu\text{g}$ ) were then migrated on a 10% (wt/vol) SDS-PAGE gel and transferred onto a nitrocellulose membrane according to the manufacturer's instructions. The Rad4 and mutant proteins levels were determined with the anti-cmyc mouse mAb 9E10 at a dilution of 1/500. The Peroxidase AffiniPure Goat Anti-Mouse IgG + IgM (H+L) (Jackson ImmunoResearch Laboratories) served as the secondary antibody, used at a dilution of 1/1,000. Loading was verified with the anti-actin mouse monoclonal antibody (Abcam) at a dilution of 1/1,000.

## **Supplementary References :**

(57) Elagoz A., Callejo M., Armstrong J., Rokeach L. A. (1999) Although calnexin is essential in *S. pombe*, its highly conserved central domain is dispensable for viability. *J. Cell Sci.* **112**, 4449–4460.

## Supplementary Tables

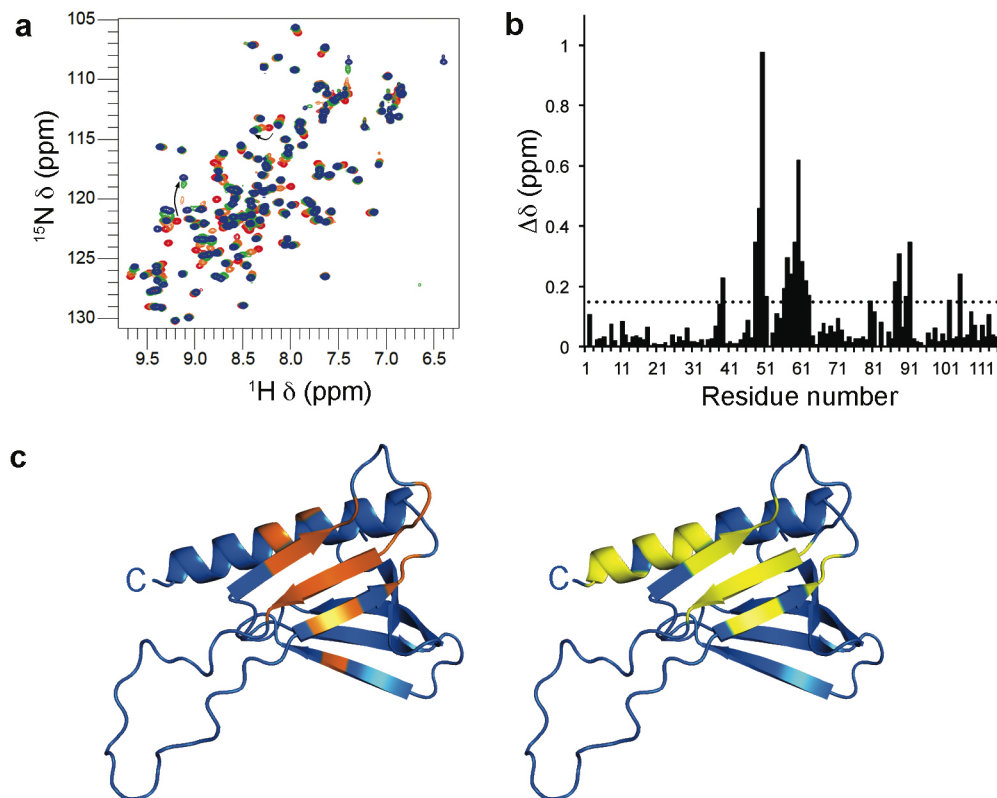
### Supplementary Table S1: Yeast strains used in this study

Name	Genotype	Source
<i>rad4</i> (6158)	Mata <i>his3Δ1 leu2Δ0 met15Δ0 ura3Δ0 rad4Δ::KanMX</i>	Open Biosystems
<i>rad4</i>	<i>rad4</i> (6158) + pRS316	This Lab
<i>RAD4</i>	<i>rad4</i> (6158) + pRS316RAD4cmyc	This Lab
<i>rad4-PP</i>	<i>rad4</i> (6158) + pRS316RAD4(F95P/V98P)cmyc	This Lab
<i>rad4-AAA</i>	<i>rad4</i> (6158) + pRS316RAD4(W649A/L652A/L656A)cmyc	This Lab
<i>rad4-PPAAA</i>	<i>rad4</i> (6158) + pRS316RAD4(F95P/V98P/W649A/L652A/L656A)cmyc	This Lab

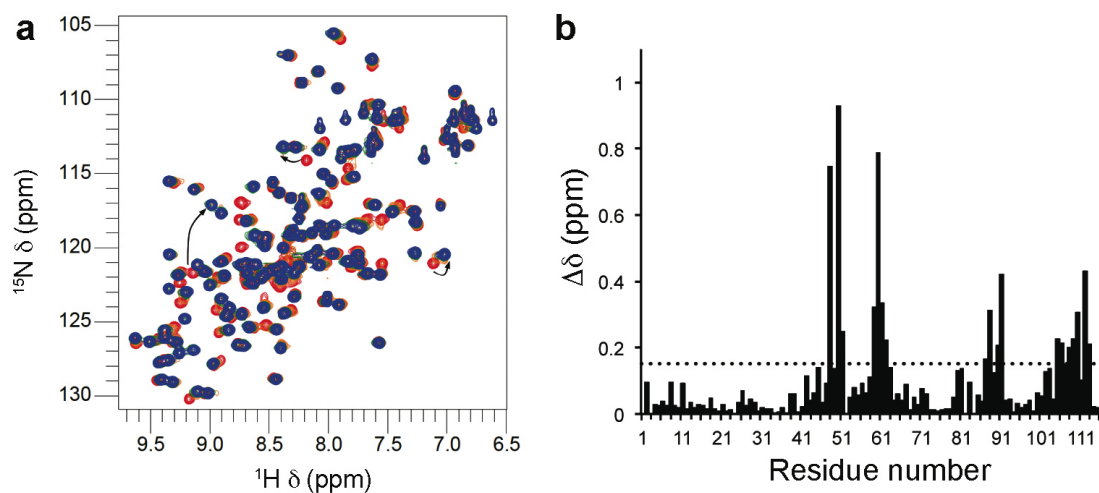
### Supplementary Table S2: Primers used in this study

Name	Sequence
pRS-RAD4-NotI-F	5' aag gaa aaa agc ggc cgc atg aaa tat gta tac ata tct tga tta act atg 3'
pRS-RAD4-EcoRI-R	5' cga att caa cta aaa tat ttc act ttg 3'
pRS-RAD4-2995-NdeI-F	5' gga att cca tat ggt aaa att gcc gag g 3'
pRS-RAD4-cmyc-R	5' cag cct cat ttc aca ggt cct cct ccg aga tca gct tct gct cgt ctg att cct ctg ac 3'
pRS-RAD4-cmyc-F	5' gtc aga gga atc aga cga gca gaa gct gat ctc gga gga cct gtg aaa tga ggc tg 3'
RAD4(F95P+V98P)-F	5' gat tcg gag gaa cct gaa gac ccg aca gat gg 3'
RAD4(F95P+V98P)-R	5' cca tct gtc ggg tct tea ggt tcc tcc gaa tc 3'
pRS-RAD4-1742-BglII-F(L)	5' gaa gat ctg act ttt taa ggg ccg tca g 3'
RAD4I(W649AL652AL656A)-R	5' ctc tcc aaa gca cca agc 3'
RAD4(W649AL652AL656A)-F	5' ctt ggt gct ttg gag agt gcg aat act gca ctg cta aaa gcg cgt att cgt agc aag ctg 3'
pRS-RAD4-EcoRI-R	5' cga att caa cta aaa tat ttc act ttg 3'

## Supplementary Figures

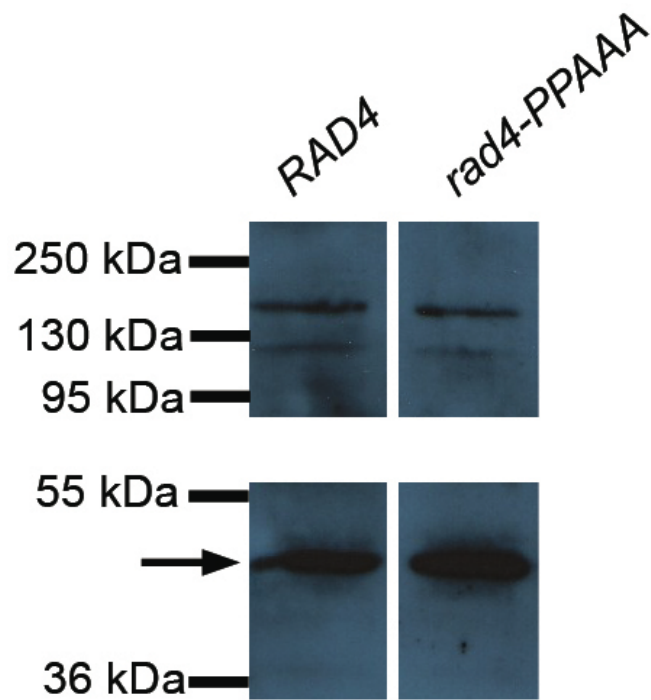


**Supplementary Figure S1. Rad4<sub>76-115</sub> binds to a similar site of Tfb1PH as Rad2<sub>642-690</sub>.** (a) Overlay of the <sup>1</sup>H-<sup>15</sup>N HSQC spectra for <sup>15</sup>N-labeled Tfb1PH in its free form (red), in the presence of 0.25 equivalents (orange), 0.5 equivalent (green) and 1 equivalent (blue) of unlabeled Rad4<sub>76-115</sub>. Arrows highlight two signals that undergo significant changes in <sup>1</sup>H and <sup>15</sup>N chemical shifts upon formation of the Rad4<sub>76-115</sub>-Tfb1PH complex. (b) Histogram of the variation in chemical shift [ $\Delta\delta_{(\text{ppm})}$ ;  $\Delta\delta = [(0.17\Delta N_H)^2 + (\Delta H_N)^2]^{1/2}$ ] observed in the <sup>1</sup>H-<sup>15</sup>N HSQC spectrum of the <sup>15</sup>N-labeled Tfb1PH upon formation of the Rad4<sub>76-115</sub>-Tfb1PH complex. (c) Ribbon models of the three dimensional structure of Tfb1PH. The amino acids showing a significant chemical shift change ( $\Delta\delta_{(\text{ppm})} > 0.15$ ) upon formation of a complex with Rad4<sub>76-115</sub> are shown in orange (left) and upon formation of a complex with Rad2<sub>642-690</sub> are shown in yellow (right).

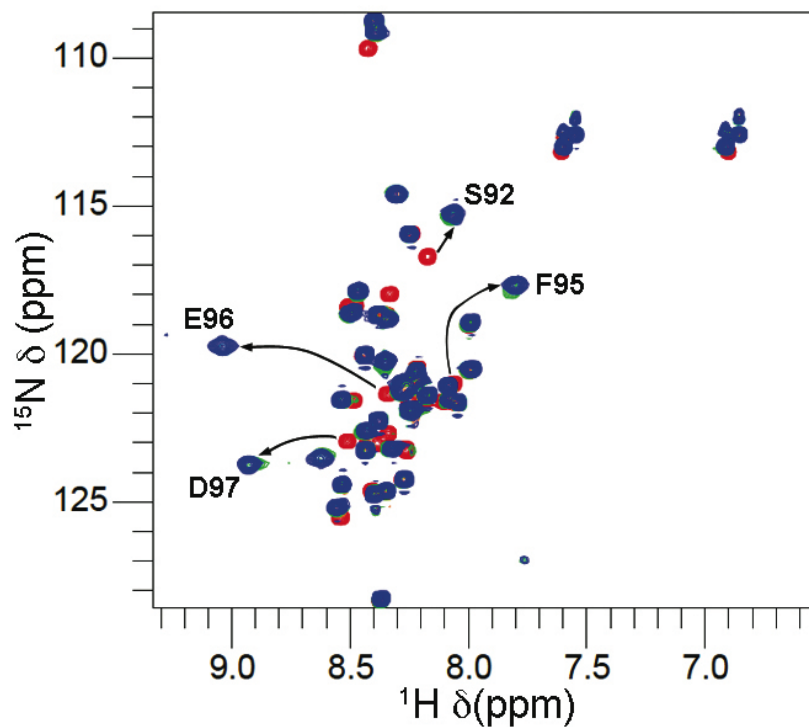


**Supplementary Figure S2. Rad34<sub>41-63</sub> binds to a similar site of Tfb1PH as Rad4<sub>76-115</sub>. (a)**

Overlay of the two dimensional <sup>1</sup>H-<sup>15</sup>N HSQC spectra for <sup>15</sup>N-labeled Tfb1PH in its free form (red), in the presence of 0.5 equivalents (orange), 0.75 equivalent (green) and 1 equivalent (blue) of unlabeled Rad34<sub>41-63</sub>. Arrows highlight several signals that undergo significant changes in <sup>1</sup>H and <sup>15</sup>N chemical shifts upon formation of the Rad34<sub>41-63</sub>-Tfb1PH complex. (b) Histogram of the variation in chemical shift [ $\Delta\delta_{(\text{ppm})}$ ;  $\Delta\delta = [(0.17\Delta N_{\text{H}})^2 + (\Delta H_{\text{N}})^2]^{1/2}$ ] observed in the <sup>1</sup>H-<sup>15</sup>N HSQC spectrum of the <sup>15</sup>N-labeled Tfb1PH upon formation of the Rad34<sub>41-63</sub>-Tfb1PH complex.

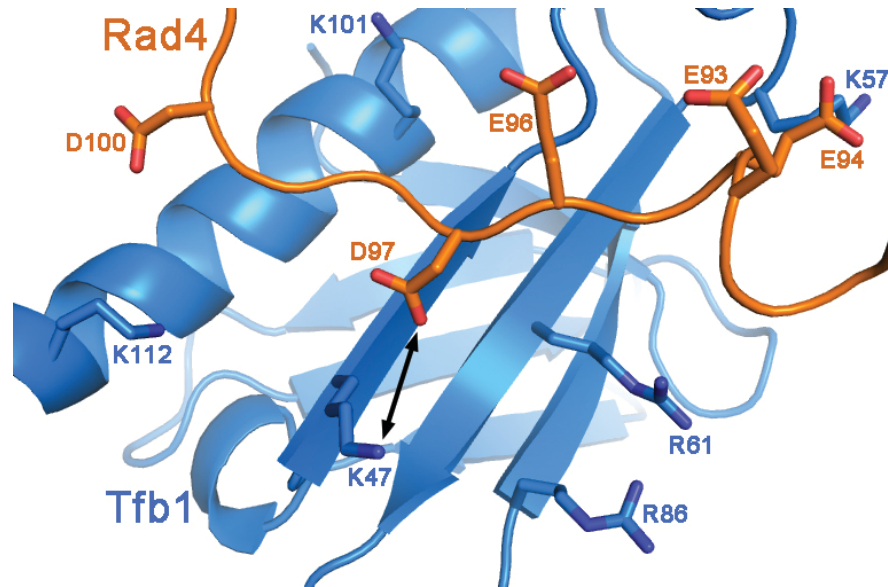


**Supplementary Figure S3. Rad4 protein expression levels in yeast.** Level of expression of the Rad4 and Rad4-PPAAA proteins in *RAD4* and *rad4-PPAAA* yeast, respectively. The protein levels were monitored by western blot with an antibody against the myc tag. Actin levels are shown as a loading control (arrow).

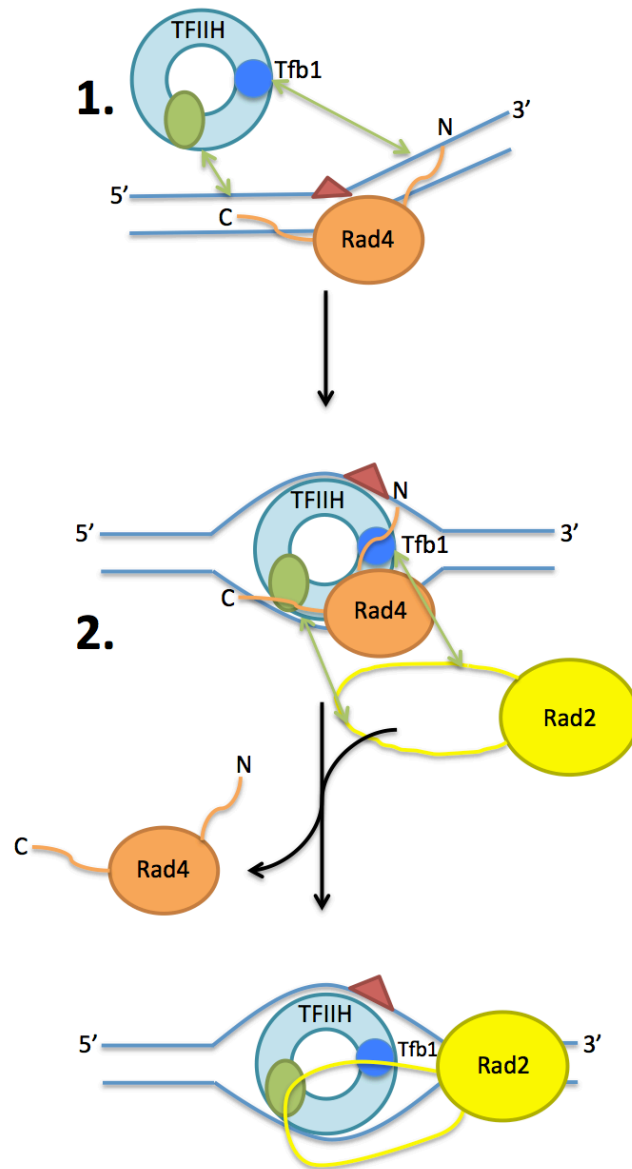


**Supplementary Figure S4. Tfb1PH binds to Rad4<sub>76-115</sub>.** Overlay of the  $^1\text{H}$ - $^{15}\text{N}$  HSQC spectra for  $^{15}\text{N}$ -labeled Rad4<sub>76-115</sub> in its free form (red), in the presence of 0.5 equivalents (orange), 0.75 equivalent (green) and 1 equivalent (blue) of unlabeled Tfb1PH. Arrows highlight several signals that undergo significant changes in  $^1\text{H}$  and  $^{15}\text{N}$  chemical shifts upon formation of the Rad4<sub>76-115</sub>-Tfb1PH complex.





**Supplementary Figure S5. The positively charged surface of Tfb1PH helps to position the negatively charged Rad4.** Ribbon representation of Tfb1PH (blue) and backbone trace of the region of Rad4<sub>76-115</sub> (orange) highlighting the positively charged residues on the surface of Tfb1PH and the negatively charged residues of Rad4. The arrow shows the potential salt bridge between Asp97 of Rad4<sub>76-115</sub> and Lys47 of Tfb1PH.



**Supplementary Figure S6. Schematic representation of the displacement of Rad4 from the repair complex by Rad2.** Rad4 (orange) recruits TFIIH to the DNA through direct interactions with either of its two TFIIH-binding motifs (N-terminal and C-terminal) (1). Rad2 (yellow) then competes with Rad4 for common binding sites on TFIIH, including Tfb1PH. It is the TFIIH-binding motifs found in its extended spacer region of Rad2 that compete with the N-terminal and C-terminal regions of Rad4 in order to displace it from the repair complex (2). The red triangle represents a damaged site on one strand of the DNA.